



Structural, magnetic and electrical properties of $\text{Bi}_{1.4}\text{La}_{0.6}\text{Sr}_2\text{CaCu}_{2-x}\text{Mn}_x\text{O}_y$ compounds

Yang Li^a, Maolin Li^a, Benzhe Sun^a, M. Babar^a, Yang Qi^{a,b,*}

^a Institute of Materials Physics and Chemistry, School of Science, Northeastern University, Shenyang 110004, PR China

^b The Key Laboratory for Anisotropy and Texture of Materials, Ministry of Education, Northeastern University, Shenyang 110004, PR China

ARTICLE INFO

Article history:

Received 7 September 2010

Received in revised form 17 January 2011

Accepted 19 January 2011

Available online 1 February 2011

Keywords:

Bi-2212

Mn-doped

Insulating character

Magnetism

ABSTRACT

The Mn-doped compounds $\text{Bi}_{1.4}\text{La}_{0.6}\text{Sr}_2\text{CaCu}_2\text{O}_y$ were prepared by sol-gel method. The structural variation was characterized systematically by X-ray diffraction (XRD), infrared (IR) spectra and Raman scattering spectra, respectively. The electrical and magnetic properties of the compounds were investigated by the temperature dependence of resistivity ($R-T$) and magnetic hysteresis loop ($M(H)$) measurements. Results indicate that the subtle change of lattice parameters has taken place in the compounds, which is attributed to CuO_2 planes canting and Mn valence alternation. In the condition of preserving Bi-2212 structure, $\text{Bi}_{1.4}\text{La}_{0.6}\text{Sr}_2\text{CaCu}_{2-x}\text{Mn}_x\text{O}_y$ compound has optimal resistivity and magnetism at $x=2\%$, which could provide a candidate as new barrier in Josephson junction in future.

© 2011 Elsevier B.V. All rights reserved.

1. Introduction

$\text{Bi}_2\text{Sr}_2\text{CaCu}_2\text{O}_y$ (Bi-2212) is a compound which exhibits superconductivity above liquid-nitrogen temperature. Compared with YBCO, it has only one kind of Cu site [1] and the oxygen deficiency during a heat cycle is very small. Therefore, it is expected that Bi-2212 system is a more appropriate candidate for the study of element substitution in Cu site. In previous studies, when Cu site was occupied by other 3d metal, such as Fe, Co, Ni, Zn and Mn, the superconducting transition temperature (T_c) of Bi-2212 system was suppressed, which was mainly due to pair-breaking effect [2–6]. The pair-breaking effect could lead to the emergence of insulating ground state, which originates from carrier localization in the vicinity of the Fermi level. Hence, the substitution of Cu by 3d metals in cuprate superconductors is indispensable.

However, the potential application of Bi-2212 insulator which is induced by element doping has not been paid much attention in the literature. In fact, insulating phase is very important in superconductor/insulator/superconductor (S/I/S) Josephson junction if it has larger resistance. In traditional Bi-2212 Josephson junction, $\text{Bi}_2\text{Sr}_2\text{CaCu}_2\text{O}_y$ (Bi-2201) is suitable for the study of S/N/S junctions, but the resistivity is not large enough to observe Josephson effects [7]. In order to improve barrier resistivity, the substitution of some rare-earth elements at Ca site could change Bi-2212 supercon-

ductor into insulator without any structural variations. Hence, $\text{Bi}_2\text{Sr}_2\text{CaCu}_2\text{O}_y/\text{Bi}_2\text{Sr}_2\text{NdCu}_2\text{O}_y/\text{Bi}_2\text{Sr}_2\text{CaCu}_2\text{O}_y$ Josephson junction with Nd substitution at Ca site has been reported by Mizuno, and a novel idea was provided about the fabrication of barrier layers in Josephson junction [8,9]. In addition to S/I/S Josephson junction, as another branch of Josephson junction, superconductor/ferromagnet/superconductor (S/F/S) Josephson junction could realize the transition of Josephson critical current between the π -state and the 0-state [10–13]. However, the F layer exhibits only very small (metallic) resistances, making this type of junctions less suitable for the study of dynamic junction properties as well as for applications, where active Josephson junctions are required. To overcome this problem, it is necessary to increase F layer resistivity. Therefore, a new superconductor/insulator/ferromagnet/superconductor (S/I/F/S) Josephson junction which has both larger resistance and magnetism was successfully fabricated by Weides and Kemmler [14], and a quantitative model of S/I/F/S Josephson junction was formulated by Vasenko [15]. Hence, the investigation of insulating character of 3d metal doped Bi-2212 system is essential and could provide an excellent insight into new barrier in Josephson junction.

In this paper, the preparation process of $\text{Bi}_{1.4}\text{La}_{0.6}\text{Sr}_2\text{CaCu}_{2-x}\text{Mn}_x\text{O}_y$ ($0 \leq x \leq 4.5\%$) compounds, where x is nominal dopant, has been optimized on the basis of our previous works [16,17]. The structural, magnetic and electrical properties of the compounds were investigated, which could provide a better understanding of Mn-doped $\text{Bi}_{1.4}\text{La}_{0.6}\text{Sr}_2\text{CaCu}_2\text{O}_y$ compounds. This compound which has both favorable insulating character and

* Corresponding author at: No. 11, Lane 3, Wenhua Road, Heping District, Shenyang, PR China. Tel.: +86 24 83683674; fax: +86 24 83683674.

E-mail address: qiyang@imp.neu.edu.cn (Y. Qi).

Table 1
Sintering temperature for different doping level of Mn.

Mn doping level x (%)	0	0.5	1.0	1.5	2.0	2.5	3.0	3.5	4.0	4.5
Sintering temperature ($^{\circ}\text{C}$)	840	845	845	848	848	852	856	860	860	866

magnetism could provide a candidate as a new barrier in Josephson junction for the future.

2. Experimental

The Mn-doped $\text{Bi}_{1.4}\text{La}_{0.6}\text{Sr}_2\text{CaCu}_{2-x}\text{Mn}_x\text{O}_y$ polycrystalline compounds were prepared by sol–gel method. $\text{Bi}(\text{NO}_3)_3 \cdot 5\text{H}_2\text{O}$, $\text{Sr}(\text{NO}_3)_2$, $\text{Ca}(\text{NO}_3)_2 \cdot 4\text{H}_2\text{O}$, $\text{Cu}(\text{NO}_3)_2 \cdot 3\text{H}_2\text{O}$, $\text{La}(\text{NO}_3)_3 \cdot 6\text{H}_2\text{O}$ and $\text{Mn}(\text{NO}_3)_2$ liquor were used as starting materials. EDTA was the chelating agent and all of the reagents were of analytical grade. The reactants were first dissolved into the de-ionized water by stirring at room temperature to yield the precursor. Then the precursor was bathed in water at 70°C in order to form gel and finally gel turns into the black powder by continuous heating. At last, the powder was sintered at different temperature for 10 h and was cooled to room temperature in the furnace, as shown in Table 1. In order to obtain the optimal effect of Mn substitution and preserve Bi-2212 structure, the sintering temperature is optimized.

For $\text{Bi}_{1.4}\text{La}_{0.6}\text{Sr}_2\text{CaCu}_{2-x}\text{Mn}_x\text{O}_y$ ($0 \leq x \leq 4.5\%$) compounds, XRD patterns were obtained using X-ray diffractometer (Rigaku-D/max, Cu-K α) with step length 0.01° . The temperature dependence of resistivity (R - T) was measured by the standard four-probe technique. The magnetic hysteresis loops (M (H))) were measured by Vibrating Sample Magnetometer (VSM, LAKE SHORE 7407). Fourier transform infrared spectra (IR) were recorded by FT-IR spectrometer (Nicolet 380). Raman scattering spectra were obtained on Raman spectrophotometer (Renishaw inVia) using a back-scattering technique, and an argon ion laser with 514.5 nm line was used as an excitation light source. All measurements were performed at room temperature, and all spectra were taken with refocusing on at least two different spots to assure reproducibility.

3. Results and discussion

The XRD patterns for $\text{Bi}_{1.4}\text{La}_{0.6}\text{Sr}_2\text{CaCu}_{2-x}\text{Mn}_x\text{O}_y$ ($0 \leq x \leq 4.5\%$) compounds are shown in Fig. 1, and the patterns can be well fitted with orthorhombic symmetry. As shown in Fig. 1(b), with increasing Mn doping level (x) until 3.5%, the peaks position (2θ) of (1 1 3), (1 1 5), (0 0 1 0), (1 1 7) and (0 2 0) shift to high-angle, which can be attributed to the Mn substitution at Cu site. As marked by the black arrow, the impurity phase of $\text{La}_{1.4}\text{Sr}_{1.6}\text{Mn}_2\text{O}_7$ emerges when $x > 3.5\%$. It could be ascribed to the substitution of Mn for Cu has been saturated, that is, no more Mn entering to Bi-2212 unit cell. The correctness of XRD results was verified by Pawley refinement, which exhibits the calculated and the experimental

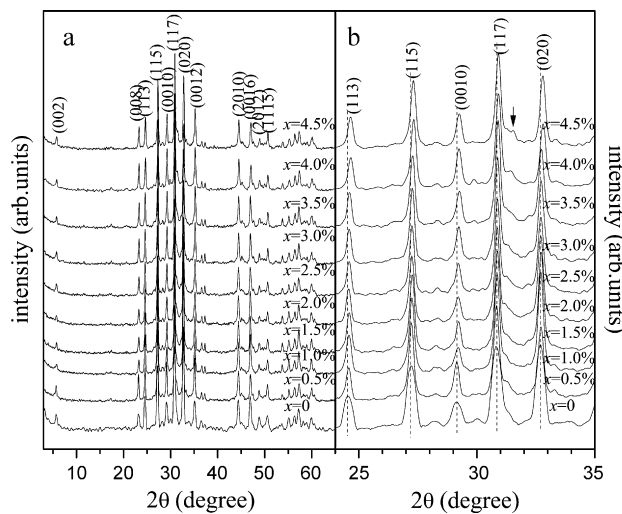


Fig. 1. X-ray powder diffraction patterns for $\text{Bi}_{1.4}\text{La}_{0.6}\text{Sr}_2\text{CaCu}_{2-x}\text{Mn}_x\text{O}_y$ ($0 \leq x \leq 4.5\%$) compounds. (a) XRD patterns ($2\theta = 3^{\circ}$ – 65°); (b) XRD patterns ($2\theta = 24^{\circ}$ – 35°); solid arrow represents $\text{La}_{1.4}\text{Sr}_{1.6}\text{Mn}_2\text{O}_7$ phase.

powder diffraction patterns together with the different plot. The Pawley refinement of $x = 4.5\%$ compound is shown in Fig. 2, which has a maximal profile residual factors (R_{wp}) of all the compounds. It is noted that all R_{wp} are smaller than 10%, indicating that the experimental data is coincident with the fitted data, which can ensure authenticity. Fig. 3 shows the lattice parameters a , b and c as a function of x . The lattice parameter a increases when x increases from 0 to 2%, and then it decreases for $x > 2\%$. At the same time the parameters b and c decrease monotonously with the increase of x . With increasing x , more oxygen entered into Bi-2212 system, which was confirmed by Sun [6]. Hence, the decrease of c is due to the increase of oxygen content in the system. The similar anomalous structural variation has also been reported in Mn-doped Bi-2201 system, which was induced by Mn aliovalent substitution [18]. However, for Mn-doped Bi-2212 system, such anomalous change has not been reported yet. There is a quantitative relationship among Mn^{3+} , Mn^{4+} and Cu^{2+} ionic radii, i.e., Cu^{2+} (0.72 \AA) = Mn^{3+} (0.72 \AA) > Mn^{4+} (0.53 \AA) [19]. Generally, the variation of lattice parameters is derived from different ionic radii. However, for the equal ionic radius of Mn^{3+} and Cu^{2+} , when x increases from 0 to 2%, the inhomologous variations of a and b suggest O–Cu–O bond angle increasing along a -axis and CuO_2 planes canting. While x exceeds 2%, the decrease of a originates from Cu–O bond shortening and the bond force enhancement. It is implied that Mn valence varies from trivalent to quadrivalent. When $x > 2\%$, a decreases and the difference between a and b becomes very small, which indicates the tendency of structural variation from orthorhombic to tetragonal symmetry.

In order to testify the conclusion deduced from the XRD patterns, infrared spectrum as an effective measurement is employed, which can reflect in-plane information of CuO_2 planes. Fig. 4(a) shows the IR spectra in the frequency range from 400 cm^{-1} to 3000 cm^{-1} at room temperature for $\text{Bi}_{1.4}\text{La}_{0.6}\text{Sr}_2\text{CaCu}_{2-x}\text{Mn}_x\text{O}_y$ compounds. A strong absorption peak can be observed obviously around 596 cm^{-1} , which can be assigned to the in-plane Cu–O stretching mode of CuO_4 “squares” [20]. With increasing x from 0 to 2%, the peak shifts down from 596 cm^{-1} to 591 cm^{-1} , then it shifts up from 591 cm^{-1} to 597 cm^{-1} for $x > 2\%$. The change of chemical bond originates from the variation of Cu–O bond force constant. In order to clearly investigate the changes, a function of absorption peak against x is given in Fig. 4(b). The absorption peak shifts down, signifying the increase of Cu–O bond length along a -axis with increasing x from 0 to 2% whereas it decreases for $x > 2\%$. The change of Cu–O bond is coincident with the variation of lattice parameter a , which provides a strong evidence that Mn valence changes from trivalent to quadrivalent. When x exceeds 4%, the absorption peak is nearly invariable, which is in accordance with above speculation that Mn has been saturated in CuO_2 planes.

The information of CuO_2 planes has been exhibited in detail through infrared spectra. And spacial structural variation can be represented well by Raman scattering spectrum as a favorable complement of IR spectra. Fig. 5 shows the Raman scattering spectra of $\text{Bi}_{1.4}\text{La}_{0.6}\text{Sr}_2\text{CaCu}_{2-x}\text{Mn}_x\text{O}_y$ ($0 \leq x \leq 3.5\%$) compounds in the frequency range of 200 – 800 cm^{-1} at room temperature. Four Raman modes around 273, 333, 559 and 599 cm^{-1} were obviously observed. As reported in Ref. [21], the 273, 333 and 599 cm^{-1} modes correspond to the B_{1g} mode of vibration of the $\text{O}(1)_{\text{Cu}}$ atoms along the c -axis, to the vibration mode of $(\text{O}_{\text{Bi}}\text{O}_{\text{Sr}})^{\text{h}}$, and to the A_{1g} mode of vibration of the $\text{O}(2)_{\text{Sr}}$ atom along the c -axis, respectively. $\text{O}(1)_{\text{Cu}}$ and $\text{O}(2)_{\text{Sr}}$ refer to oxygen atoms in the CuO_2 and SrO layer. The peak appears around 559 cm^{-1} , assigned as the A_{1g} stretch mode of O atom along c -axis, which belongs to the La–O bond [22].

It can be observed that the $\text{O}(1)_{\text{Cu}}$ B_{1g} and the $(\text{O}_{\text{Bi}}\text{O}_{\text{Sr}})^{\text{h}}$ mode around $273/333\text{ cm}^{-1}$ almost retain constant with increasing x from 0 to 3.5%. In order to investigate the multi-peak clearly, the peak has been divided into two parts. As shown in Fig. 6, the frequency

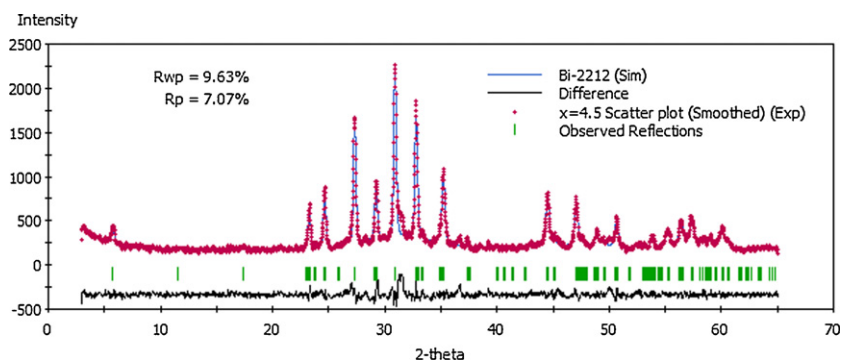


Fig. 2. Pawley refinement of $\text{Bi}_{1.4}\text{La}_{0.6}\text{Sr}_2\text{CaCu}_{2-x}\text{Mn}_x\text{O}_y$ sample at $x=4.5\%$.

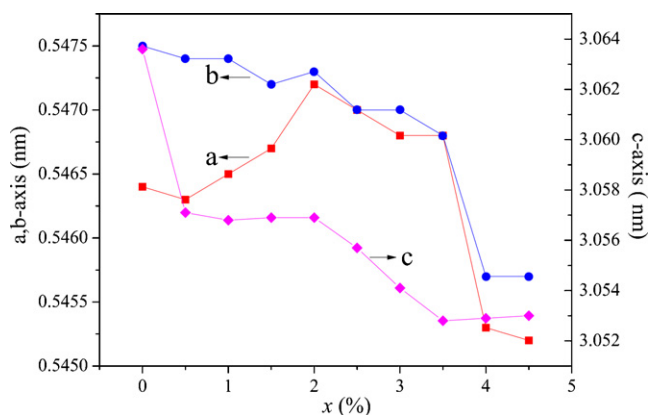


Fig. 3. The lattice parameters a , b and c as a function of x for $\text{Bi}_{1.4}\text{La}_{0.6}\text{Sr}_2\text{CaCu}_{2-x}\text{Mn}_x\text{O}_y$ ($0 \leq x \leq 4.5\%$) compounds.

of $O(2)_{\text{Sr}}$ phonon pair shifts up slightly from 599 cm^{-1} to 602 cm^{-1} as x increases from 0 to 1.5%, then it shifts down to 593 cm^{-1} when x is equal to 2%. The slight up-shift of $O(2)_{\text{Sr}}$ mode may be due to stronger bond force of Mn^{3+} than Cu^{2+} ions, while the down-shift can be explained by the expansion of $\text{Cu}-\text{O}_{\text{Sr}}$ bond length, which is induced by the increase of $\text{O}-\text{Cu}-\text{O}$ bond angle along a -axis and CuO_2 planes canting. When $x > 2\%$, the frequency of $O(2)_{\text{Sr}}$ phonon pair shifts up from 593 cm^{-1} to 600 cm^{-1} . This phenomenon is due to the substitution of Mn^{4+} for Cu^{2+} ions, because Mn^{4+} has smaller ionic radius as well as strong $\text{Mn}-\text{O}$ bond force constant. The trend of $O(2)_{\text{Sr}}$ A_{1g} mode reflects not only the CuO_2 planes canting but

also the change of Mn valence from trivalent to quadrivalent, which is coincident with the conclusions deduced from XRD patterns. The variation of $O A_{1g}$ mode of $\text{La}-\text{O}$ bond and the intensity of two peaks may relate to the distance between layers in $\text{Bi}-2212$ system. The downshift of $O A_{1g}$ mode may reveal the increase of distance in Bi_2O_2 and SrO layer, which could result in larger $\text{Bi}-\text{O}_{(\text{Sr})}$ bond polarizability and phonon intensity, leading to the variation of relative intensity of two peaks.

On the basis of above analysis, the XRD pattern manifests that Mn atoms are successfully entered into $\text{Bi}_{1.4}\text{La}_{0.6}\text{Sr}_2\text{CaCu}_{2-x}\text{Mn}_x\text{O}_y$ compounds. The variation of lattice parameter implies that the substitution of Mn for Cu results in Mn valence alternation and CuO_2 planes canting with increasing x , confirmed by infrared and Raman scattering spectra. In addition to structural variation, the physical properties can also be influenced significantly by Mn doping. In order to investigate the effect of Mn doping on $\text{Bi}_{1.4}\text{La}_{0.6}\text{Sr}_2\text{CaCu}_{2-x}\text{Mn}_x\text{O}_y$ compounds systematically, the study of resistivity measurement is indispensable.

As shown in Fig. 7, all the samples show the negative temperature coefficient of resistivity with $d\rho/dt < 0$, indicating that the insulating behavior is shown in $\text{Bi}_{1.4}\text{La}_{0.6}\text{Sr}_2\text{CaCu}_{2-x}\text{Mn}_x\text{O}_y$ ($0 \leq x \leq 3.5\%$) compounds. With the increase of x from 0 to 2%, the resistivity increases gradually with increasing CuO_2 planes canting except for $x=1.5\%$, then it decreases as well as CuO_2 planes canting for $x > 2\%$. Combined with structural analysis, variation of resistivity is derived from CuO_2 planes canting. The abnormal variation of resistivity emerges at $x=1.5\%$ due to the decrease of CuO_2 planes canting, which is confirmed by Raman scattering spectrum, as shown in Fig. 6(c). It has been reported that the variation of resistivity was neither due to lattice site vacancies nor oxygen content, but due to $3d$ element substitution at Cu site [2]. Based on the study

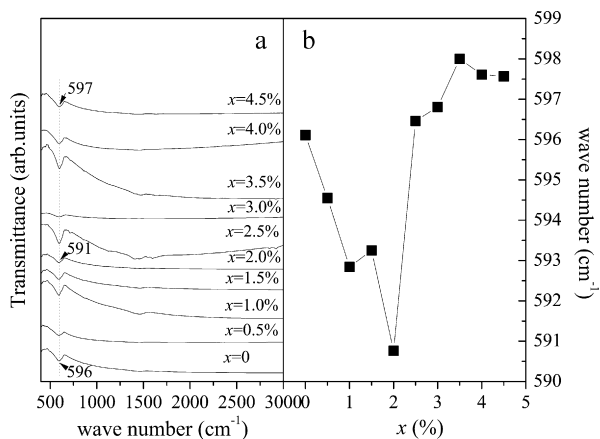


Fig. 4. Infrared spectra of $\text{Bi}_{1.4}\text{La}_{0.6}\text{Sr}_2\text{CaCu}_{2-x}\text{Mn}_x\text{O}_y$ ($0 \leq x \leq 4.5\%$) compounds. (a) Infrared spectra; (b) absorption peak with different Mn doping levels, plotted as wave number vs. x .

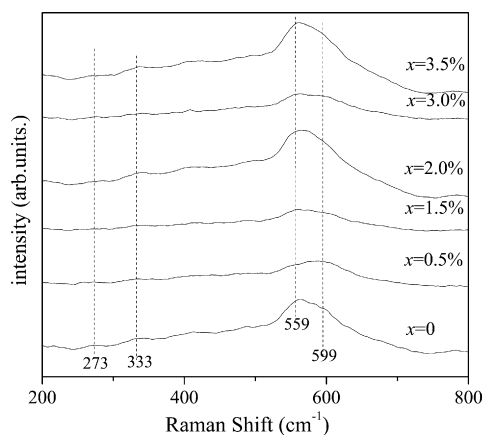


Fig. 5. Raman scattering spectra of $\text{Bi}_{1.4}\text{La}_{0.6}\text{Sr}_2\text{CaCu}_{2-x}\text{Mn}_x\text{O}_y$ ($0 \leq x \leq 3.5\%$) compounds.

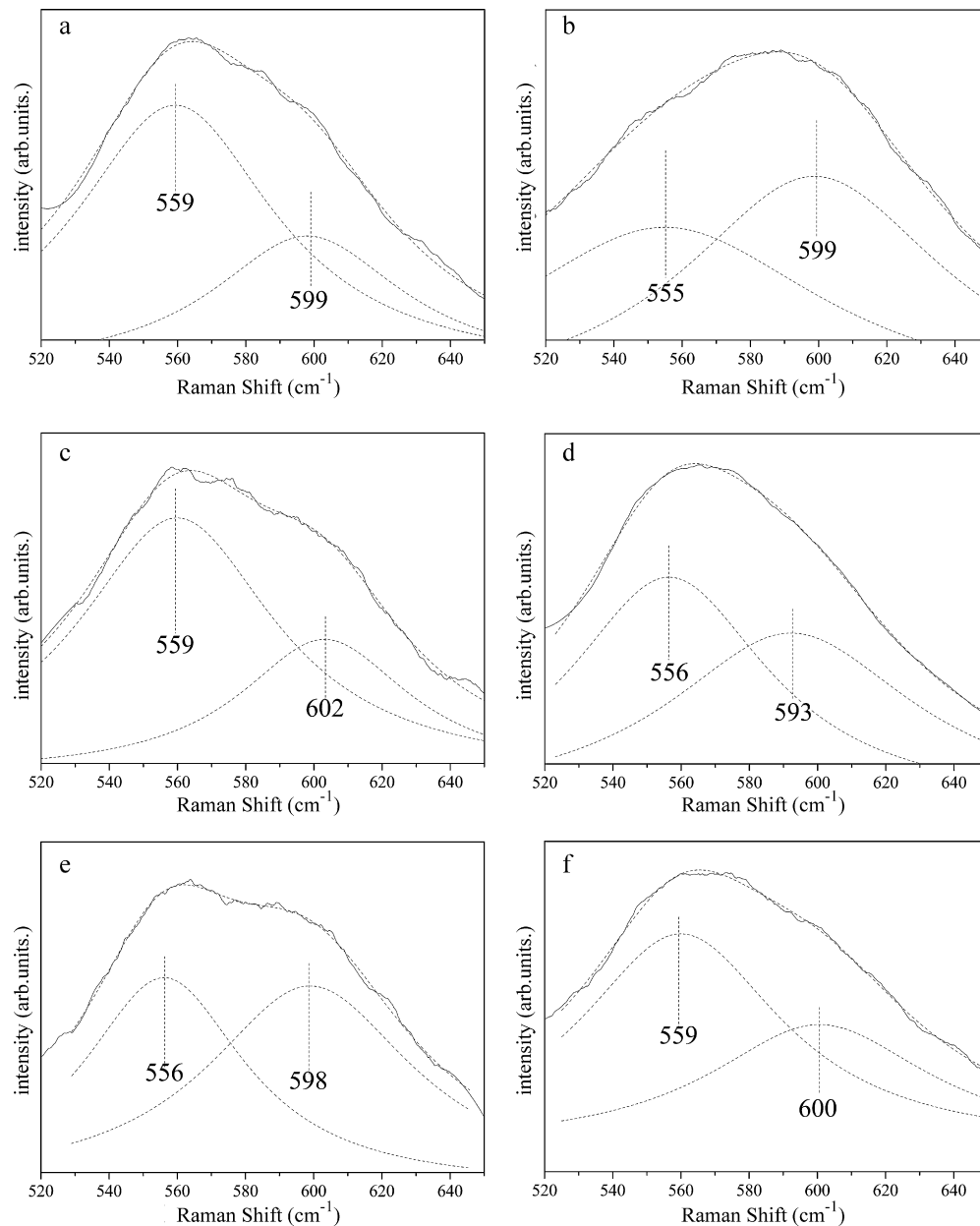


Fig. 6. The divided peak of $\text{Bi}_{1.4}\text{La}_{0.6}\text{Sr}_2\text{CaCu}_{2-x}\text{Mn}_x\text{O}_y$ ($0 \leq x \leq 3.5\%$) compounds. The solid line is experimental data, and the dash line is generated data.

of Mn-doped $\text{Bi}_{1.4}\text{La}_{0.6}\text{Sr}_2\text{CaCu}_2\text{O}_y$ compounds, it may be inferred by the competition between carrier localization and magnetic scattering, induced by Mn doping. And the mechanism is needed to be further investigated in details.

In order to testify magnetic variation in $\text{Bi}_{1.4}\text{La}_{0.6}\text{Sr}_2\text{CaCu}_{2-x}\text{Mn}_x\text{O}_y$ compounds, $M(H)$ at room temperature are given in Fig. 8. With increasing x from 0 to 2%, the remanent magnetization (M_r) increases whereas decreases for $x > 2\%$. The increase of M_r suggests that magnetism increases when x increases from 0 to 2%. However, the decrease of M_r provides strong evidence that Mn valance changes from trivalent to quadrivalent when $x > 2\%$. At low temperature, the enhancement of magnetization may be resulted from the disappearance of thermal perturbation.

According to analysis of R-T and $M(H)$ curves, insulating character and magnetism can coexist in $\text{Bi}_{1.4}\text{La}_{0.6}\text{Sr}_2\text{CaCu}_{2-x}\text{Mn}_x\text{O}_y$ compounds. As shown in Fig. 7, the resistivity is about 10^2 (Ωmm) at room temperature and can reach 10^5 (Ωmm) at low temperature for $x=2\%$. However, the resistivity of Bi-2201 compound

is about 10^{-1} (Ωmm) at room temperature [23], which is not low enough to be an insulating barrier. In order to attain a high-quality tunneling type device, a barrier with larger resistivity is necessary. In addition to the barrier in S/I/S Josephson junction, a new multiple barrier which has both large resistance and magnetism has been successfully fabricated recently in S/I/F/S Josephson junction [24–26]. In S/I/F/S Josephson junction, a damped oscillation of the superconducting order parameter in F-layer is induced by the proximity effect in ferromagnetic layer. Josephson phase μ transformed from 0 to π in $I_s = I_c \sin(\mu)$ is realized by controlling the thickness of F-layer. However, there is still no such report for Bi-2212 SIFS Josephson junction. As an excellent insulator, along with preserving Bi-2212 structure, having relatively strong magnetism, maximum resistivity at room temperature which is higher than that of Bi-2201 about 3 orders are characteristic of $\text{Bi}_{1.4}\text{La}_{0.6}\text{Sr}_2\text{CaCu}_{2-x}\text{Mn}_x\text{O}_y$ compound at $x=2\%$. It is considered that the I/F multi-layers in S/I/F/S Josephson junction may be replaced by such a single layer. Hence, this com-

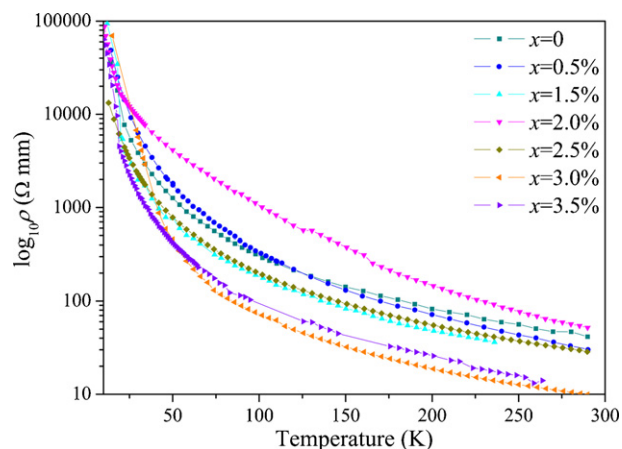


Fig. 7. R–T curves of $\text{Bi}_{1.4}\text{La}_{0.6}\text{Sr}_2\text{CaCu}_{2-x}\text{Mn}_x\text{O}_y$ compounds. $x=0$, squares; $x=0.5\%$, circles; $x=1.5\%$, up triangles; $x=2.0\%$, down triangles; $x=2.5\%$, diamond; $x=3.0\%$, left triangles; $x=3.5\%$, right triangles. The ρ is plotted in log 10 scale.

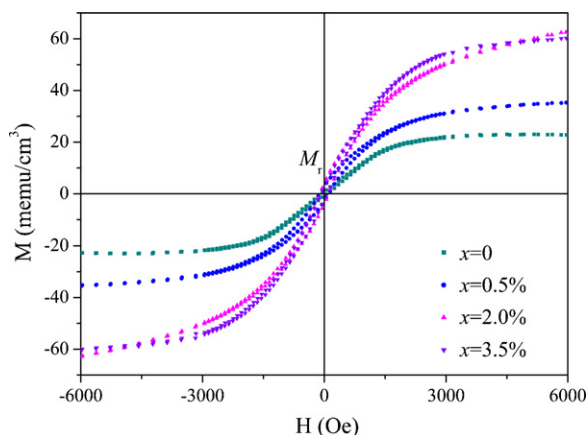


Fig. 8. Magnetic hysteresis loop of $\text{Bi}_{1.4}\text{La}_{0.6}\text{Sr}_2\text{CaCu}_{2-x}\text{Mn}_x\text{O}_y$ compounds at room temperature. $x=0$, squares; $x=0.5\%$, circles; $x=2\%$, up triangles; $x=3.5\%$, down triangles.

compound could provide a candidate as a new barrier in Josephson junction in future. In next works, the fabrication and application of $\text{Bi}_2\text{Sr}_2\text{CaCu}_2\text{O}_y/\text{Bi}_{1.4}\text{La}_{0.6}\text{Sr}_2\text{CaCu}_{2-x}\text{Mn}_x\text{O}_y/\text{Bi}_2\text{Sr}_2\text{CaCu}_2\text{O}_y$ Josephson junction will be our major subject.

4. Conclusions

Based on the experimental data, Mn has successfully entered into $\text{Bi}_{1.4}\text{La}_{0.6}\text{Sr}_2\text{CaCu}_2\text{O}_y$ compounds. The variation of lattice parameter implies O–Cu–O bond angle increasing along a -axis and CuO_2 planes canting when x increases from 0 to 2%. As x increases from 2 to 3.5%, Mn valence varies from trivalent to quadrivalent. The impurity phase of $\text{La}_{1.4}\text{Sr}_{1.6}\text{Mn}_2\text{O}_7$ emerges when $x > 3.5\%$, indicating that no more Mn enters into Bi-2212 unit cell which suggests

that the substitution of Mn for Cu has saturated in CuO_2 planes. The investigation of infrared and Raman scattering spectra confirms the conclusions deduced from calculation of lattice parameter. The insulating character is exhibited in R–T, which is affected significantly by CuO_2 planes canting. $M(H)$ manifests that magnetism exists in the compounds. In summary, under the circumstance of preserving Bi-2212 structure, $\text{Bi}_{1.4}\text{La}_{0.6}\text{Sr}_2\text{CaCu}_{2-x}\text{Mn}_x\text{O}_y$ compound has optimal resistivity and magnetism at $x=2\%$, which could provide a candidate as new barrier in Josephson junction in future.

Acknowledgements

Financial support for this work was provided by the National Science Foundation of China (Grant Nos. 50572013 and 10874022) and the Doctoral Program Foundation of the Education Ministry (Grant No. 20070145092).

References

- [1] J.M. Tarascon, Y. LePage, P. Barboux, B.G. Bagley, L.H. Greene, W.R. McKinnon, G.W. Hull, M. Giroud, D.M. Huang, *Phys. Rev. B* 37 (1988) 9832.
- [2] A. Maeda, T. Tabe, S. Takebayashi, M. Hase, K. Uchi-nokura, *Phys. Rev. B* 41 (1990) 4112.
- [3] B. von Hedt, W. Lisseck, K. Westerholt, H. Bach, *Phys. Rev. B* 49 (1994) 9898.
- [4] M. Boekholt, Th. Bollmeier, L. Buschmann, M. Fleuster, G. Güntherodt, *Physica C* 198 (1992) 33.
- [5] P. Sumana Prabhu, M.S. Ramachandra Rao, G.V. Subba Rao, *Physica C* 211 (1993) 279.
- [6] X.F. Sun, X. Zhao, L. Wang, Q.F. Zhou, W.B. Wu, X.-G. Li, *Physica C* 324 (1999) 193.
- [7] K. Mizuno, H. Higashino, K. Setsune, K. Wasa, *Appl. Phys. Lett.* 58 (1991) 640.
- [8] K. Mizuno, K. Setsune, *Jpn. J. Appl. Phys.* 30 (1991) L1559.
- [9] K. Mizuno, H. Higashino, K. Setsune, *Supercond. Sci. Technol.* 9 (1996) A129.
- [10] T. Kontos, M. Aprili, J. Lesueur, F. Genêt, B. Stephanidis, R. Boursier, *Phys. Rev. Lett.* 89 (2002) 137007.
- [11] Thierry Champel, Tomas Löfwander, Matthias Eschrig, *Phys. Rev. Lett.* 100 (2008) 077003.
- [12] C. Gürllich, S. Scharinger, M. Weides, H. Kohlstedt, R.G. Mints, E. Goldobin, D. Koelle, R. Kleiner, *Phys. Rev. B* 81 (2010) 094502.
- [13] Mohammad Alidoust, Jacob Linder, Gholamreza Rashedi, Takehito Yokoyama, Asle Sudbø, *Phys. Rev. B* 81 (2010) 014512.
- [14] M. Weides, M. Kemmler, E. Goldobin, D. Koelle, R. Kleiner, H. Kohlstedt, A. Buzdin, *Appl. Phys. Lett.* 89 (2006) 122511; M. Kemmler, M. Weides, M. Weiler, M. Opel, S.T.B. Goennenwein, A.S. Vasenko, A.A. Golubov, H. Kohlstedt, D. Koelle, R. Kleiner, E. Goldobin, *Phys. Rev. B* 81 (2010) 054522.
- [15] A.S. Vasenko, A.A. Golubov, M.Yu. Kupriyanov, M. Weides, *Phys. Rev. B* 77 (2008) 134507.
- [16] Ying Zhang, Maolin Li, Huazhe Yang, Yang Qi, *J. Northeast. Univ. (Nat. Sci.)* 29 (2008), 11.
- [17] Zhuangzhi Zhi, Ying Zhang, Maolin Li, Bingsen Zhang, Benzhe Sun, Ning He, Yang Qi, *Rare Met. Mater. Eng.* 37 (Suppl. 4) (2008) 201.
- [18] Jianwu Zhang, Weixian Wang, Changjin Zhang, Eue-Soon Jang, Jin-Ho Choy, Yuheng Zhang, *Physica C* 419 (2005) 85.
- [19] R.D. Shannon, *Acta Crystallogr. A* 32 (1976) 751.
- [20] R. Henn, A. Wittlin, M. Cardona, S. Uchida, *Phys. Rev. B* 56 (1997) 6295.
- [21] M. Kakihana, M. Osada, M. Kall, L. Borjesson, H. Mazaki, H. Yasuoka, M. Yashima, M. Yoshimura, *Phys. Rev. B* 53 (1996) 11796.
- [22] D.B. Romero, V.B. Podobedov, A. Weber, J.P. Rice, J.F. Mitchell, R.P. Sharma, H.D. Drew, *Phys. Rev. B* 58 (1998) R14737.
- [23] Gaojie Xu, Qirong Pu, Zejun Ding, Yuheng Zhang, *Physica C* 340 (2000) 178.
- [24] M. Weides, C. Schindler, H. Kohlstedt, *J. Appl. Phys.* 101 (2007) 063902.
- [25] M. Weides, H. Kohlstedt, R. Waser, M. Kemmler, J. Pfeiffer, D. Koelle, R. Kleiner, E. Goldobin, *Appl. Phys. A* 89 (2007) 613.
- [26] Shiro Kawabata, Yasuhiro Asano, Yukio Tanaka, Alexander A. Golubov, Satoshi Kashiwaya, *Phys. Rev. Lett.* 104 (2010) 117002.